# A Probability Description of the Yule-Nielsen Effect II: The Impact of Halftone Geometry

**J. S. Arney and Miako Katsube**

*Center for Imaging Science, Rochester Institute of Technology, Rochester, New York 14623*

The Yule-Nielsen effect, also called optical dot gain, has often been modeled based on convolutions between halftone dot patterns and a point spread function PSF characteristic of the paper. An alternative approach to modeling the Yule-Nielsen effect employs probability functions that describe the fraction of reflected light emerging between halftone dots and under dots. The probability model is shown to fit experimental data on the Yule-Nielsen effect for a variety of different types of halftone geometries, including both AM and FM halftones. The particular form of the functions is shown to be dependent on the halftone geometry, but all forms examined contained a parameter $w$, which is a quantitative index of the magnitude of the Yule-Nielsen effect. The $w$ parameter in all cases was shown to be related exponentially to the MTF constant $k_p$ of the paper.

## Introduction

The reflectance $R$ of a halftone image is governed by the reflectance of the paper $R_p$, the reflectance of the ink dot $R_i$, the fraction of the area of the image covered with dots $F$, and the degree of lateral scatter of the light in the paper. The lateral scatter of light in the paper is often called the Yule-Nielsen effect. As shown previously, the relationship between $F$, $R_p$, and $R_i$ is well modeled by the Murray-Davies Eq. 1,

$$R = FR_i + (1 - F)R_p, \tag{1}$$

and the Yule-Nielsen effect causes the ink and paper reflectances $R_i$ and $R_p$ to decrease as $F$ increases.[1,2] In the previous report, the variation of $R_i$ and $R_p$ with $F$ was modeled based on a probability function $P_p$, which described the probability that a photon will emerge under a halftone dot after entering the paper between halftone dots.[2] The previous study involved application of the probability model to tone reproduction in traditional clustered halftone dots. The current report extends the probability model to other types of halftones including disperse dots, error diffusion, and similar FM systems. Assumptions made in the model and experimental tests of the model are: (1) no penetration of the dot into the paper occurs, (2) the halftone dots obey the Beer-Lambert law, and (3) negligible contribution from total internal reflection occurs between dots and paper. Variation from these three assumptions will be the subject of later studies. This study is concerned with the impact of halftone geometry on the probability function $P_p$.

## Background

The earliest halftone model to account for the Yule-Nielsen effect assumed $R_i$ and $R_p$ to be constants and employed[3–5] an empirical power factor $n$ as a modification to Eq. 1.

$$R(F) = [FR_i^{1/n} + (1 - F)R_p^{1/n}]^n. \tag{2}$$

Equation 2, called the Yule-Nielsen equation, often does a very good job of modeling tone reproduction, but the physical significance of the n power factor is not entirely clear. Moreover, Eq. 2 does not describe the way in which $R_i$ and $R_p$ vary with $F$. Thus, other strategies for modeling the effect have been investigated and reported in the literature. The most fundamental modeling approach is a convolution between the geometric pattern of the halftone dots $G(x,y)$ and the point spread function (PSF) of light in paper.[6–9] This requires knowledge of the PSF of paper or the corresponding MTF in the Fourier domain. The MTF of the paper may be modeled empirically as follows:

$$MTF(\omega) = \frac{1}{1 + (k_p\omega)^2}, \tag{3}$$

where $k_p$ is proportional to the average distance light travels laterally before emerging from the paper and $\omega$ is the spatial frequency in the Fourier domain.[10]

An alternative tone reproduction model is based on probability functions for lateral motion of light in paper.[2,11,12] Instead of modeling the MTF or PSF of the paper, a probability function $P_p$ is modeled to describe the probability that a photon that enters the paper between the halftone dots will emerge under a halftone dot. Conceptually $P_p$ can be derived from PSF. However, the PSF function of paper is typically modeled empirically, so empirically modeling $P_p$ serves as a somewhat simpler starting point. As described previously,[2] this probability function governs the reflectance of the paper between the halftone dots,
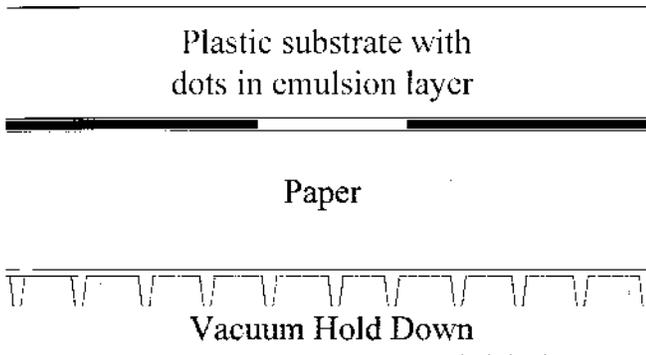
**Figure 1.** Schematic of film-based halftone dots in contact with paper using a vacuum hold down.

$$R_p = R_g[1 - P_p(1 - T_i)], \tag{4}$$

where $R_g$ and $T_i$ are the reflectance of the not-printed paper and the transmittance of the printed ink, respectively. Both $R_g$ and $T_i$ are constants independent of $F$.

The $P_p$ function is also related to the probability $P_i$ that a photon that enters the paper by first passing through a halftone dot also returns under the dot. The relationship between the two probabilities was shown to be

$$\tag{5}$$

from which the reflectance of the halftone dot may be calculated.[2]

$$R_i = R_gT_i[1 - P_i(1 - T_i)]. \tag{6}$$

The overall reflectance of the halftone image is then calculated with Eq. 1. Thus, knowledge of the constants $R_g$ and $T_i$ and of the probability function, $P_p$ yields a tone reproduction model of $R$ versus $F$. The key part of the model is a knowledge of the probability function $P_p$.

### The $P_p$ Function and AM Halftone Dots

The previous study suggested the following empirical model for $P_p$ for a clustered dot, AM halftone,[2]

$$P_p = F[1 - (1 - F)^w + (1 - F^w)], \tag{7}$$

where $w$ is an empirical power factor. By selecting a value for $w$, the $P_p$ function may be used sequentially in Eqs. 4, 5, 6, and 1 to calculate reflectances $R_i$, $R_p$, and $R$ versus dot area fraction $F$. The value of $w$ is selected to provide the best fit between the model and experimental data.

An experimental test of this halftone model was made by placing halftone patterns, formed on high-contrast photographic film, into vacuum contact with paper as shown in Fig. 1. As described earlier,[12] the film halftones were generated with a commercial graphic arts image setter. The resulting halftone image was then examined with a microdensitometer as described previously,[1,2] and the reflectance of the paper between the dots $R_p$ and the mean reflectance $R$ were measured directly. Figure 2 illustrates data for halftones at 3.3 and 5.2 dot/mm (85 and 133 lpi) on noncoated paper. The halftone film dots have a density above 2.0 allowing the approximation $R_i = 0$, thus simplifying the analysis. The value of $w$ was adjusted to fit the
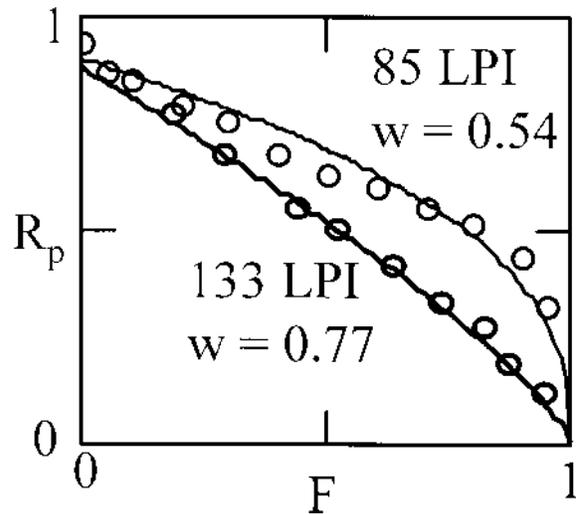


**Figure 2.** Experimental values of $R_p$ versus $F$ for AM halftone gray scales at $f = 3.3$ and 5.2 dot/mm (85 and 133 lpi) on noncoated paper of $k_p = 0.449$ mm$^{-1}$. The lines through the data are the model with $w = 0.54$ and 0.77 using the model of Eqs. 7, 4 and 1.
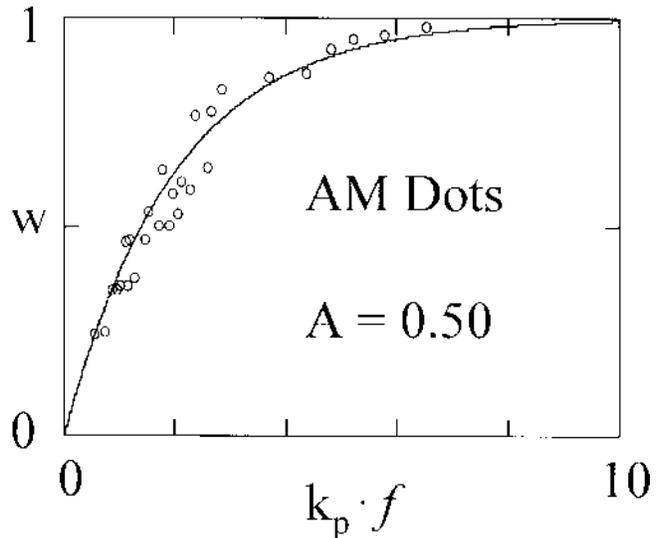


**Figure 3.** Measured values of $w$ versus the product of the halftone frequency $f$ in dot/mm and the paper MTF constant $k_p$ in mm$^{-1}$ for AM halftones in vacuum contact with papers of various $k_p$.

data on $R_p$ versus $F$, as illustrated in Fig. 2. The experiment was repeated with AM halftone patterns ranging from $f = 2.6$ to $f = 5.9$ dot/mm (65 to 150 lpi). The experiment was also performed with several papers, both coated and noncoated, having MTF constants ($k_p$ in Eq. 3) over the range 0.2 mm $< k_p <$ 1.0 mm, as determined in an earlier project.[10] Figure 3 shows the relationship between the values of $w$, determined by fitting the model to the data, and the product $k_pf$. As described previously, the relationship between $w$ and $k_pf$ may be approximated[13] closely by the exponential function of Eq. 8.

$$w = 1 - e^{-Ak_pf}. \tag{8}$$

The value of $A$ is chosen to provide the best fit between Eq. 8 and the experimental data in Fig. 3. For the AM clustered dot halftone, a value of $A = 0.5$ provides a good fit to the data.
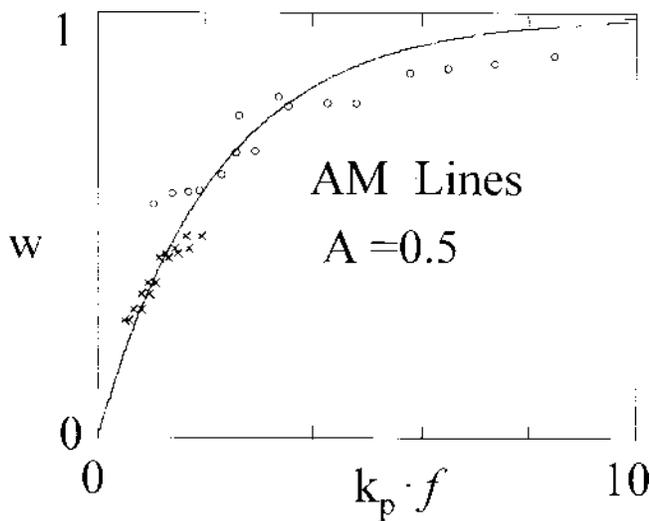
**Figure 4.** Measured $w$ versus $k_p f$ for AM halftone lines: x are coated papers and ○ noncoated papers.

## The $P_p$ Function and AM Halftone Lines

The $w$ parameter is an index of the magnitude of the Yule-Nielsen effect, and Eq. 8 provides a quantitative relationship between $w$ and the $k_p$ of the paper and the halftone dot frequency $f$. One may speculate the value of $A$ is related to the type of geometric pattern $G(x,y)$, of the halftone pattern. To test this hypothesis, halftones of different geometric patterns were generated on film and measured exactly as described above. One type of pattern examined was the AM halftone line.[13] This is a halftone in one dimension $G(x)$ rather than two $G(x,y)$. The line frequency varied over the range $2.4 < f < 7.7$ lpm (60 to 195 lpi), and at each line frequency the image reflectance $R$ was controlled as a function of the width of the halftone line. As the line width increased, $F$ increased, resulting in a decrease in $R$, just as with traditional halftone dots.

The films containing the halftone lines were placed in contact with the coated and noncoated papers as before, and measurements were made of $R_p$ and $R$ versus $F$ at each line frequency $f$. Equations 7, 4, and 1 were fit to the experimental values of $R_p$ and $R$ versus $F$. The resulting values of $w$ were then plotted as shown in Fig. 4 and compared with Eq. 8 at $A = 0.5$. No difference between the halftone dots and the AM lines could be detected experimentally.

## The $P_p$ Function and FM Halftone Dots

Stochastic halftones, produced by a proprietary error diffusion algorithm, were also examined to determined the utility of the probability model for tone reproduction with this type of halftone. The algorithm for generating this type of halftone involves varying the frequency of occurrence of square dots with dots remaining at a constant size. Thus the FM halftone varies $F$ by varying $f$ at a fixed dot area, while the AM halftone varies $F$ by varying dot area at a fixed $f$. Figure 5 illustrates the stochastic halftone with the physical size of the dot labeled $\lambda$.

The stochastic halftones were generated on film and were placed in vacuum contact with the paper samples as before. Experimental measurements of $R_p$ and $R$ were again measured, and the model of Eqs. 7, 4, and 1 applied as shown in Fig. 6. In this case the fit between the data and the model was not good, especially for the $R_p$ data. The problem was anticipated to be the probability function $P_p$ of Eq. 7. By trial and error, the following function for $P_p$ was found to provide an excellent fit between the data and the model, as illustrated in Fig. 7.

$$P_p = w \, [1 - (1 - F)^B]. \tag{9}$$

The most notable difference between the AM systems and the FM stochastic system is that $R_p$ does not tend toward zero in the FM system but levels out to a finite value as $F$ approaches zero. This occurs because, as illustrated in Fig. 5, the size of the halftone "hole" remains constant as $F$ approaches unity, and the "holes" simply move farther and farther apart as $F$ approaches unit. The reflectance of the paper in this "hole" thus reaches a constant value greater than zero.

Stochastic halftones at different dot sizes $\lambda$ were also measured, as illustrated in Fig. 8. It was observed that all fit the model of Eqs. 9, 4, and 1, with the same value of $B = 1.2$ but with $w$ values that increased as $\lambda$ decreased. All combinations of halftone $\lambda$ with papers of different $k_p$ were measured, and in every case $B = 1.2$ and the relationship between $w$ and $k_p/\lambda$ was found to follow a function analogous to Eq. 8, as illustrated in Fig. 9.

$$w = 1 - e^{-A k_p / \lambda}. \tag{10}$$

## The $P_p$ Function and FM Halftone Lines

One-dimensional FM halftones were also examined, but their behavior was found to be much different from the FM dots. Figure 10 illustrates the FM lines generated on film for this project. If the linewidth $\lambda$ is maintained constant, then the space between the lines decreases progressively toward zero. The spaces behave more like AM halftones, and indeed the measured behavior of $R_p$ versus $F$, shown in Fig. 11, is closer to the AM model of Eq. 7 than to the FM model of Eq. 9. Measurements of $w$ versus $k_p/\lambda$ were made, as before, and found to fit well with Eq. 10 with a value of $A = 0.24$, as shown in Fig. 12.
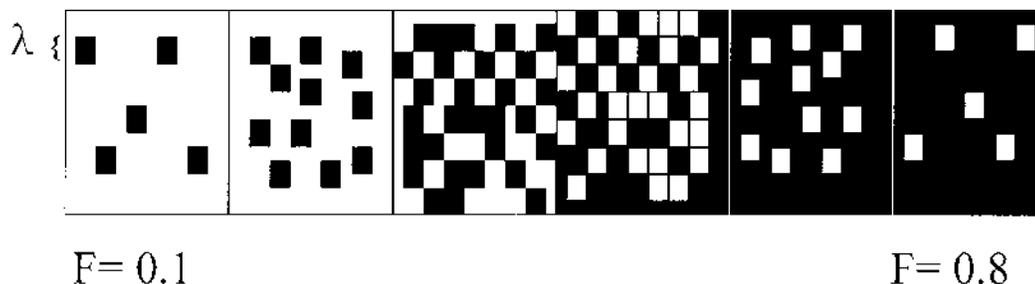


**Figure 5.** Illustration of stochastic FM halftone dot pattern. The dots are square with sides of length $\lambda$.
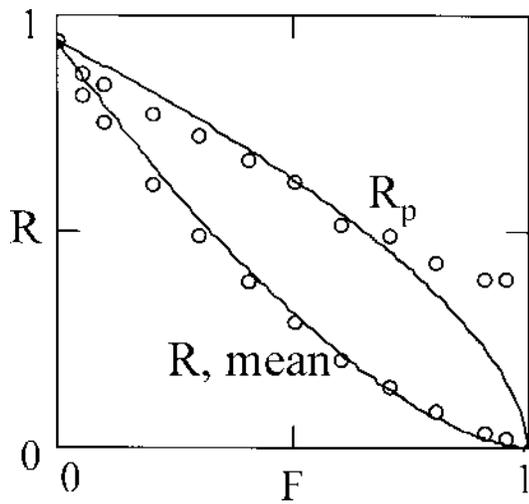
**Figure 6.** The values $R_p$ and $R$ versus $F$ for stochastic halftones with dots of $\lambda = 0.133$ mm on noncoated paper of $k_p = 0.449$ mm$^{-1}$, fit with the model of Eqs. 7, 4 and 1.
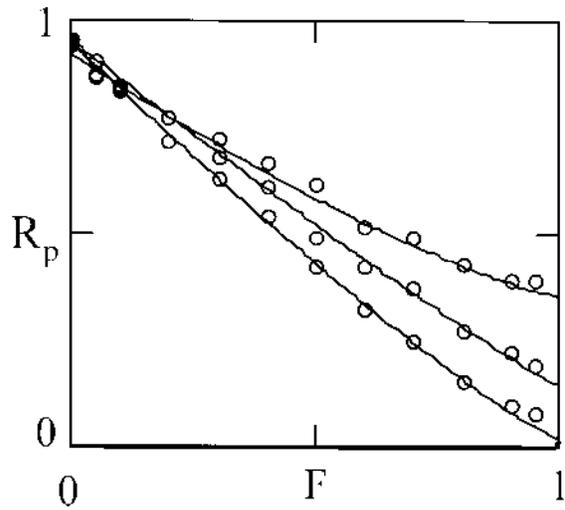


**Figure 8.** The value $R_p$ versus $F$ for stochastic halftones of $\lambda = 0.133$, 0.063, and 0.021 mm (top to bottom) on noncoated paper of $k_p = 0.449$ mm$^{-1}$, fit with the model of Eqs. 9, 4 and 1 for $w = 0.61$, 0.85, and 0.95 (top to bottom) and $B = 1.2$ for all.
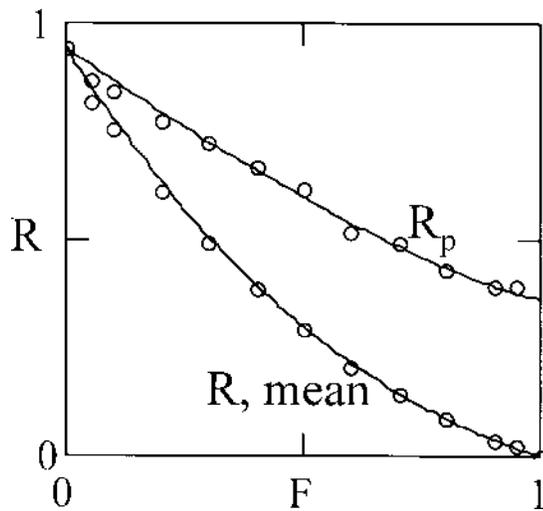


**Figure 7.** The values $R_p$ and $R$ versus $F$ for stochastic halftones with dots of $\lambda = 0.133$ mm on noncoated paper of $k_p = 0.449$ mm$^{-1}$, fit with the model of Eqs. 9, 4 and 1, $w = 0.61$ and $B = 1.2$.
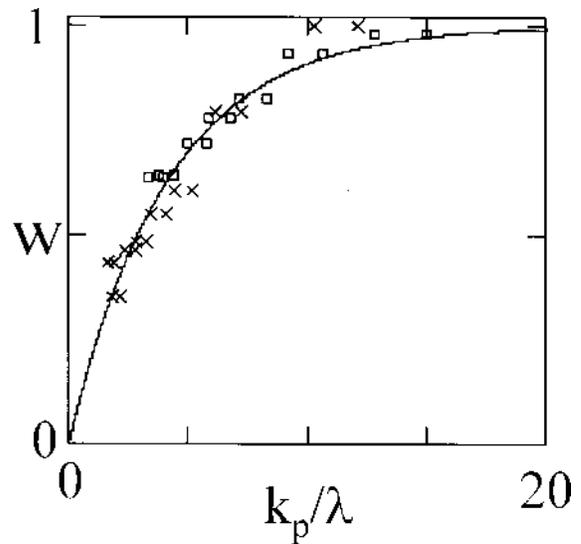


**Figure 9.** Measured $w$ versus $k_p/\lambda$ for stochastic FM halftone dots, fit with Eq. 10 at $A = 0.24$. x are coated and □ noncoated papers.
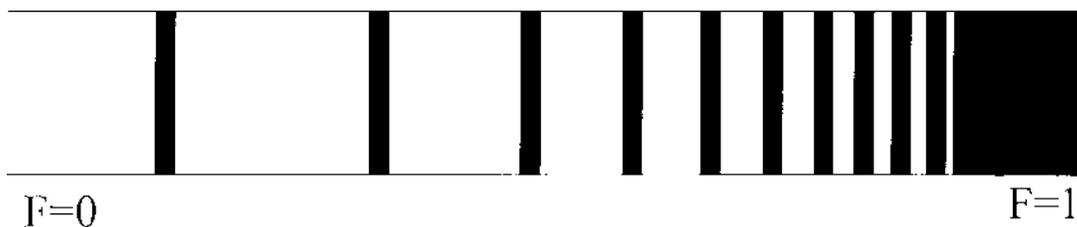


**Figure 10.** Illustration of a halftone line pattern that is FM in terms of the lines, but AM with respect to the spaces between the lines.
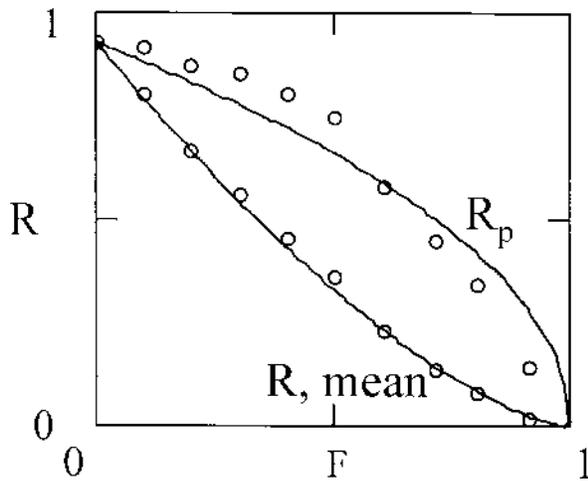
**Figure 11.** The value $R_p$ versus $F$ for an FM line halftone with $\lambda$ = 0.053 mm in vacuum contact with a paper of $k_p$ = 0.449 mm$^{-1}$.
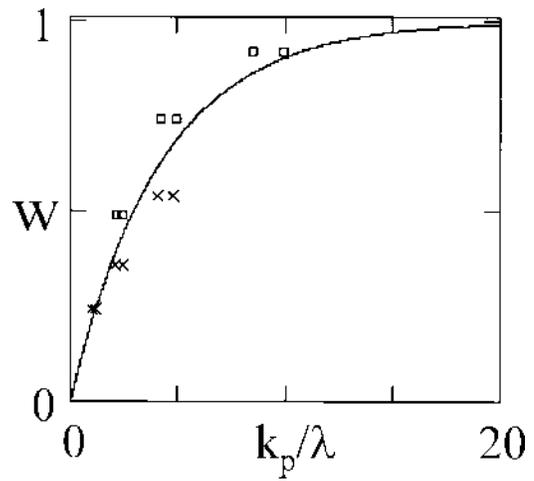


**Figure 12.** Measured $w$ versus $k_p/\lambda$ for FM halftone lines, fit with Eq. 10 at $A$ = 0.24: x are coated and □ noncoated papers.



F=1        F=0

**Figure 13.** Illustration of a halftone line pattern that is FM in terms of the spaces between the lines, but AM with respect to the lines.
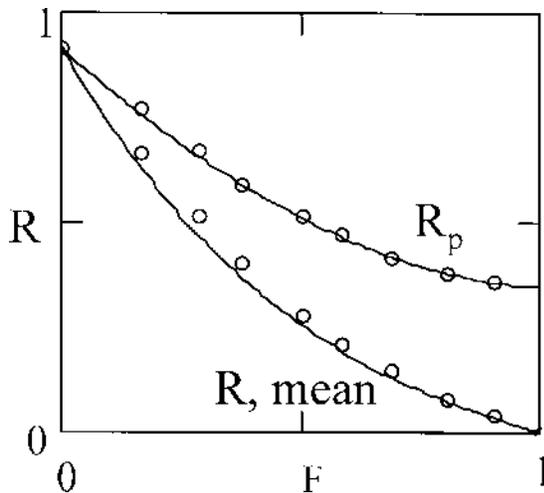


**Figure 14.** The value $R_p$ versus $F$ for an FM space halftone with $\lambda$ = 0.212 mm in vacuum contact with a paper of $k_p$ = 0.449 mm$^{-1}$.
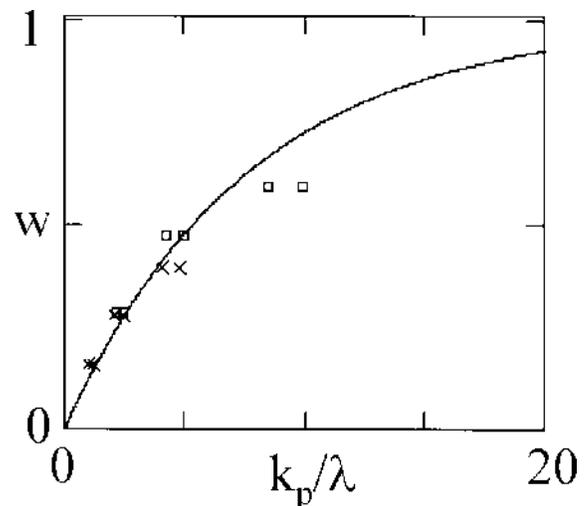


**Figure 15.** Measured $w$ versus $k_p/\lambda$ for FM halftone spaces, fit with Eq. 10 at $A$ = 0.24: x are coated and □ noncoated papers.

Another set of one-dimensional FM halftones was constructed as illustrated in Fig. 13. These FM halftones are FM with regard to the space between the lines. The spaces are of a fixed $\lambda$ with varying frequency of occurrence of the spaces. In this case, as illustrated in Fig. 14, the behavior is much like the FM stochastic halftone and fits well with Eqs. 9, 4, and 1. Moreover, all of the halftone gray scales constructed with FM spaces were fit with the same value of $B$ = 2.0 and $w$ versus $k_p/\lambda$ was well fit by Eq. 10 at $A$ = 0.13, as shown in Fig. 15.

**Conclusion**

The probability model of halftone behavior is not really a different model from the PSF/MTF models already published by other researchers. Rather, the probability model is an empirical simplification. The paper PSF is the fundamental probability function describing lateral light scatter, and the $P_p$ functions should be derivable from a convolution of the dot geometries with the PSF. However, because the PSF is typically modeled empirically, building a halftone model starting with an empirically derived

**TABLE I. Summary of $P_p$ Functions and Values of Parameters A and B for the Geometric Halftone Patterns Used in the Current Study**

| Halftone geometry | A | B | $P_p$ Equation |
|---|---|---|---|
| AM line | 0.5 | — | 7 |
| AM dot | 0.5 | — | 7 |
| FM line | 0.24 | — | 7 |
| FM space | 0.13 | 2.0 | 9 |
| Stochastic | 0.24 | 1.2 | 9 |

$P_p$ function is reasonable. The thrust of the current work is to show some useful $P_p$ models for different halftone geometries and how they relate to the PSF/MTF through the empirical $k_p$ constant.

The probability model of the Yule-Nielsen halftone effect appears applicable experimentally to halftones of any type by selecting the appropriate function for $P_p$. Table I above summarizes the results for the cases examined in this project. In all cases, a $w$ parameter can be defined within the $P_p$ function that characterizes the magnitude of the Yule-Nielsen effect. In all cases, the $w$ parameter is related exponentially to the paper MTF constant $k_p$ and either $\lambda$ for FM halftones or $f$ for AM halftones. The values of $A$ and $B$ are characteristic of the particular geometric pattern used to form the halftones.

Three simplifying assumptions were made in this study: $T_i = 0$, perfect hold-out, and zero internal reflection between the dots and the paper. All three are of considerable practical interest and will be examined in future studies. The first two are reasonable assumptions to make with the experimental film systems used in this study, but the assumption that no internal reflection exists is perhaps significantly far from the truth.[11] If, however, multiple internal reflections have a significant effect on the film halftones, the effect is the same for all of the halftone geometries in this study. Thus, the values of $A$ and $B$ may depend not only on the geometry of the halftones $G(x,y)$, but also on the degree of internal reflection between the halftones and the paper. Differences in $A$ and $B$ between patterns, then, may be considered relative differences due to differences in halftone geometry. Evidence that internal reflections may be significant in the current study can be found in the experimental value $A = 0.5$ for the AM halftone lines. A previous study of the theoretical behavior of AM lines derived[13] a value of $A = 0.66$. The difference between this theoretical value and the value observed with the film halftones may indeed be the result of multiple reflections between the film and the paper. Such reflections would increase the mean free path $k_p$ of the light, thus making the experimental data plot with a lower value of $A$.

The potential utility of a probability model of halftones is in its simplicity. Models based on PSF convolution with the halftone geometry $G(x,y)$ are intrinsically cumbersome computationally. Moreover, more complex three-dimensional geometries such as ink penetration into the paper, nonuniform ink coverage, physical dot gain, etc., make convolution models still more cumbersome to implement. Huntsman[11] and Maltz,[12] for example, have shown the probability approach as more amenable to complex systems. Future studies will examine the utility of the current probability approach to modeling more complex halftone systems. ◭

## References

1. J. S. Arney, P. G. Engeldrum, and H. Zeng, *J. Imag. Sci, Technol.* **39,** 502 (1995).
2. J. S. Arney, *J. Imag. Sci. Technol.* **41,** 633 (1997).
3. A. Murray, *J. Franklin Inst.* **221,** 721 (1936).
4. J. A. Yule and W. J. Nielsen, *TAGA Proc.* (1951) p. 65.
5. F. R. Clapper and J. A. Yule, *J. Opt. Soc. Amer.* **43,** 600 (1953).
6. F. Ruckdeschel and O. G. Hauser, *Appl. Opt.* **17,** 3376 (1978).
7. M. Wedin and B. Kruse, *Proc. SPIE,* **2413,** (1995).
8. B. Kruse and M. Wedin, *TAGA Proc.* 329 (1995).
9. S. Gustavson, *Proc. of IS&T Conference on Digital Printing*, IS&T, Springfield, VA, 1996, p. 111
10. J. S. Arney, C. D. Arney, M. Katsube, and P. G. Engeldrum, *J. Imag. Sci. Technol.* **40,** 19 (1996).
11. J. R. Huntsman, *J. Imag. Tech.* **13,** 136 (1987).
12. M. Maltz, *J. Appl. Photogr. Eng.* **9,** 83 (1983).
13. J. S. Arney, C. D. Arney, and P. G. Engeldrum, *J. Imag. Sci. Technol.* **40,** 233 (1996).